In-situ deposition of MOF-74(Cu) nanosheet arrays onto carbon cloth to fabricate a sensitive and selective electrocatalytic biosensor and its application in the determination of glucose in human serum

Shuisheng Hu [1,a,b], Yuxia Lin [1,a], Jing Teng [c,*], Wing-Leung Wong [b,*], Bin Qiu [a,*]

[a] Ministry of Education Key Laboratory for Analytical Science of Food Safety and Biology, Fujian Provincial Key Laboratory of Analysis and Detection for Food Safety, Fuzhou University, Fuzhou, Fujian, 350108, P. R. China.

[b] The State Key Laboratory of Chemical Biology and Drug Discovery and Department of Applied Biology and Chemical Technology, The Hong Kong Polytechnic University, Hung Hom, Kowloon, Hong Kong, SAR, P. R. China.

[c] Department of Laboratory, Xiamen Hospital of Traditional Chinese Medicine, Xiamen Hospital, Beijing University of Chinese Medicine, Xiamen TCM Hospital Affiliated to Fujian University of Traditional Chinese Medicine.

* Corresponding author:

E-mail: summer328cn@163.com (B. Qiu);

E-mail: tengjing1108@163.com (J. Teng);

E-mail: wing.leung.wong@polyu.edu.hk (W.-L. Wong);

[1] These authors contributed equally to this work.

Tel: +86-591-22866135

Abstract

A new electrocatalytic biosensor (MOF-74(Cu) NS-CC) based on the *in-situ* deposition of MOF-74(Cu) nanosheet on carbon cloth via a bottom-up synthetic approach in a glass tube was developed. The electrocatalytic activity of the deposited MOF-74(Cu) NS was demonstrated in the oxidation of glucose to gluconate under alkaline conditions. Our results revealed that the method of *in-situ* formation of MOF-74(Cu) NS onto a carbon cloth surface in a multi-layer solution is able to generate a stable MOF-74(Cu) NS-CC electrode with excellent sensing performance. When the as-synthesized MOF-74(Cu) NS-CC was applied directly as the working electrode for glucose sensing, it showed much higher conductivity and redox-activity than MOF-74(Cu) NS-GCE. With the potential applied at 0.55 V (vs Ag/AgCl), this new electrocatalytic biosensor exhibits an excellent linear relationship between the current density and the concentration of glucose. Moreover, a wide linear range of detection (1.0 to 1000 μM) was observed. The limit of detection was found to be 0.41 μM (S/N=3). The response sensitivity calculated is 3.39 mA mM^{-1} cm^{-2} when the concentration of glucose is in the range of 1-80 μM and 3.81 mA mM^{-1} cm^{-2} for the concentration at 100-1000 μM. This study provides a low-cost, easy to prepare and reproducible methodology for the synthesis of highly redox-active nanomaterials based on the in-situ formation of two-dimensional MOF-74(Cu) NS for the development of new electrocatalytic biosensors.

Introduction

Metal-organic frameworks (MOFs) are multi-functional materials that have great plasticity in nano-engineering to create unique functionality and are widely applied in a broad areas of material science [1], [2], [3], [4] and sensing [5,6]. Some recent developments of MOFs have extended their applications in electrocatalysis and electroanalysis because a number of advantages could be achieved by integrating MOFs to develop new materials for these important applications. MOFs are porous crystalline materials and may act as host substrates for the immobilization of catalysts, such as nanoparticles and enzymes [7,8]. Moreover, MOFs can be used as the sacrificial templates for calcinations into metallic or carbonaceous nanomaterials to produce the structurally defined electrocatalysts [9-11]. However, most investigations find that MOFs suffer from some critical limitations, such as hindered active sites and poor electron transfer that significantly reduce the redox-activity of the catalyst [12]. These adverse factors may restrict the potential application of MOFs in the field of electrocatalysis and electroanlysis and thus further advancement is required.

Recently, two-dimensional (2D) MOFs have been demonstrated to generate special structures that are able to offer tailor-made chemical and physical properties. The 2D-MOFs also possess many highly accessible active sites on the surface, which is significant for the applications in electrocatalysis [13] and electrosensing [14] as the redox-activity of the metallic sites in the 2D-MOF materials can be enhanced [15]. Therefore, many new generations of electrosensor have been fabricated with 2D MOFs such as NCST-1 ($[Co(DCTP)(L)(H_2O)_2]_n$) [14]. Most nanomaterial-based electrochemical sensors are currently fabricated through the modification of nanomaterials and followed immobilizing them with nafion onto the surface of the working electrode [16,17]. This process for assembling of sensing systems is time consuming and also causes significant drawbacks. In particular, for the immobilization of nanomaterials that have low conductivity, nafion usually causes higher resistance of the composites than that of the pure nanomaterial. The activity of the nanomaterial is therefore significantly reduced in the applications of electrocatalysis and electrosensing. The recent developments have shown that direct growth (*in-situ* deposition) of nanomaterials onto the surface of some conductive substrates, such as carbon cloth (CC), metal foam (nickel foam and copper foam) and indium tin oxide glass (ITO), as the working electrode is able to overcome the problem. This strategy for nanomaterials deposition is a recognized method

to enhance the catalyst–substrate interaction for efficient electron transport during the electrocatalytic reactions [18]. Recently, many studies have been reported on the growth of 3D-MOF onto a surface of conductive substrates for electrocatalytic applications. For example, MOF-74(Co,Fe)/Co nanosheet was *in-situ* deposited to the surface of carbon cloth to form Co,Fe-MOF-74/Co/CC. The material was applied as hybrid electrode for water splitting in alkaline condition [19]. In addition, the 2D-MOF with a conductive substrate was also fabricated, such as the core-shell Co_3O_4/Ni-MOFs NS that was deposited to the surface of carbon cloth by a facile two-step hydrothermal strategy to form Co_3O_4/Ni-MOFs-CC. The material was demonstrated as supercapacitor in alkaline and near-infrared photocatalytic hydrogen evolution [20]. However, no example of electrocatalytic biosensing system developed with *in-situ* deposition of 2D-MOFs onto the surface of conductive substrate has been reported thus far.

Our previous studies demonstrated that copper-based MOFs can be developed as the sensitive and selective biosensors for rapid detection of biologically important analysts [21]. Monitoring glucose levels in blood is a very essential part of managing diabetes because glucose is an important biological analyst for clinical diagnosis [22,23]. To develop catalysts with high activity and selective to promote the catalytic oxidation of glucose is important in the field of biofuel cells[24] and nonenzymatic sensors [25,26]. Up to now, various precious transition metals and their complexes have shown very good electrocatalytic activity towards nonenzyme glucose oxidation [27,28]. However, to further improve their electrical conductivity, redox-activity and sensitivity, most of these electrocatalytic glucose-sensing systems are developed based on nanomaterial-carbon nanotubes or grapheme composites. To advance further these sensing systems for practical and wider applications, a facile protocol for surface deposition or immobilization of electrocatalysts to achieve excellent conductivity and redox-activity is crucial [29-31].

In the present study, a new copper-based MOF nanosheet (MOF-74(Cu) NS) was synthesized under room temperature conditions via a bottom-up synthesis strategy. The *in-situ* fabricated MOF-74(Cu) NS-CC electrode applying Cu(II) ions as the metal node, which is also the active site for electrocatalysis, was used directly (no further calcination is required) as the nonenzymatic electrosensor for direct determination of glucose contents in human blood or serum samples. The

synthesized materials of MOF-74(Cu) NS and MOF-74(Cu) NS-CC were fully characterized by TEM, SEM, AFM, XPS, XRD, FTIR and BET. The electrocatalytic activity, selectivity, sensitivity, and stability of the new MOF-74(Cu) NS-CC electrosensor towards glucose in alkaline media were also investigated.

2. Experimental section

2.1 Reagents and instruments

Sodium hydroxide (0.1 M in water), copper nitrate trihydrate ($Cu(NO_3)_2 \cdot 3H_2O$), 2,5-dihydroxyterephthalic acid (DHTP), N,N-dimethylformamide (DMF), acetonitrile, ethanol, glucose (Glu), ascorbic acid (AA), fructose (Fru), lactose (Lac) and uric acid (UA), HQ, CTH, Ca^{2+}, Mg^{2+} were purchased from Aladdin (Shanghai, China). Carbon cloth was purchased from Wuhan Gaoss Union technology Co., Ltd. Human serum was obtained from Xiamen Hospital of Traditional Chinese Medicine. All chemicals and solvents used were analytical grade. The de-ionized water (18.2 MΩ cm) used was from a Milli-Q water purification system.

2.2 Synthesis of MOF-74(Cu) NS-CC

Firstly, a piece of carbon cloth (Ø=1.2 cm) was pre-cleaned by sonication in diluted hydrochloric acid (3 M), acetone and ethanol, pre-cleaned carbon cloth was dried at 333 K under vacuum condition. The PTFE seal tape was torn into thin lines and passing through the middle of the carbon cloth, paper clip was used as a pendant to suspend the carbon cloth in the linker layer. The solutions for *in-situ* growth of MOF-74(Cu) NS onto carbon cloth surface was prepared as described in supporting Information for the synthesis of MOF-74(Cu) NS.

2.3 Fabrication of MOF-74(Cu) NS-CC the working electrode

MOF-74(Cu) NS-CC (1.0×0.5 cm) was directly applied as working electrode for electrochemical tests, in which a Pt wire was used as the counter electrode and using Ag/AgCl electrode was a reference electrode. A MOF-74(Cu) NS-GCE was prepared with MOF-74(Cu) NS and using nafion (0.5 wt%) as the binder to deposit onto the surface of a glassy carbon electrode (GCE). In order to compare the glucose determination performance between MOF-74(Cu) NS-CC and MOF-

74(Cu) NS-GCE, MOF-74(Cu) NS-GCE was also fabricated by following the previous reported procedures [32].

2.4 Electrochemical testing

The amperometric *i-t* curve was carried out for the determination of glucose in 10 mL NaOH aqueous solution (0.1 M). To this NaOH aqueous solution the glucose solution (10 μL) at different concentration was added. The current signal at 0.55 V (vs Ag/AgCl) of the oxidation of glucose for each addition was recorded by the electrochemical work station (CHI660).

3. Results and Discussion

3.1 Characterization of MOF-74(Cu) NS and MOF-74(Cu) NS-CC

The synthesis of MOF-74(Cu) NS-CC was conducted in a glass tube, as shown in Fig. S1, using multi-layer of solutions for the *in-situ* formation of MOF-74(Cu) NS onto the carbon cloth surface. The as-synthesized materials were characterized with SEM and TEM. Fig. 1A and B show the SEM images of MOF-74(Cu) NS-CC. The images indicate that MOF-74 (Cu) NS was grown evenly on the surface. Fig. 1C shows clearly that the morphology of MOF-74 (Cu) NS is the honeycomb-like nanosheet arrays. As indicated from the AFM image of MOF-74 (Cu) NS shown in Fig. S2, the thickness of the nanosheet is about 4.5 nm. Moreover, Fig. 1D reveals that the MOF-74(Cu) NS was an ultra-thin nanosheet. From Fig. 1E, the EDS mapping images of MOF-74 (Cu) NS-CC, it reveals an extremely homogeneous distribution of Cu, O and C in MOF-74 (Cu) NS-CC. The characterization of MOF-74(Cu) NS was investigated in detail with XPS, XRD, FT-IR and BET (Fig. S3-S4). These characterization results support evidently the *in-situ* formation of MOF-74(Cu) NS on carbon cloth.

The XPS survey spectra and high-resolution XPS spectra of MOF-74 (Cu) NS were shown in Fig. S2. The results show that MOF-74 (Cu) NS contains Cu, C and O elements. The Cu2P spectra shows

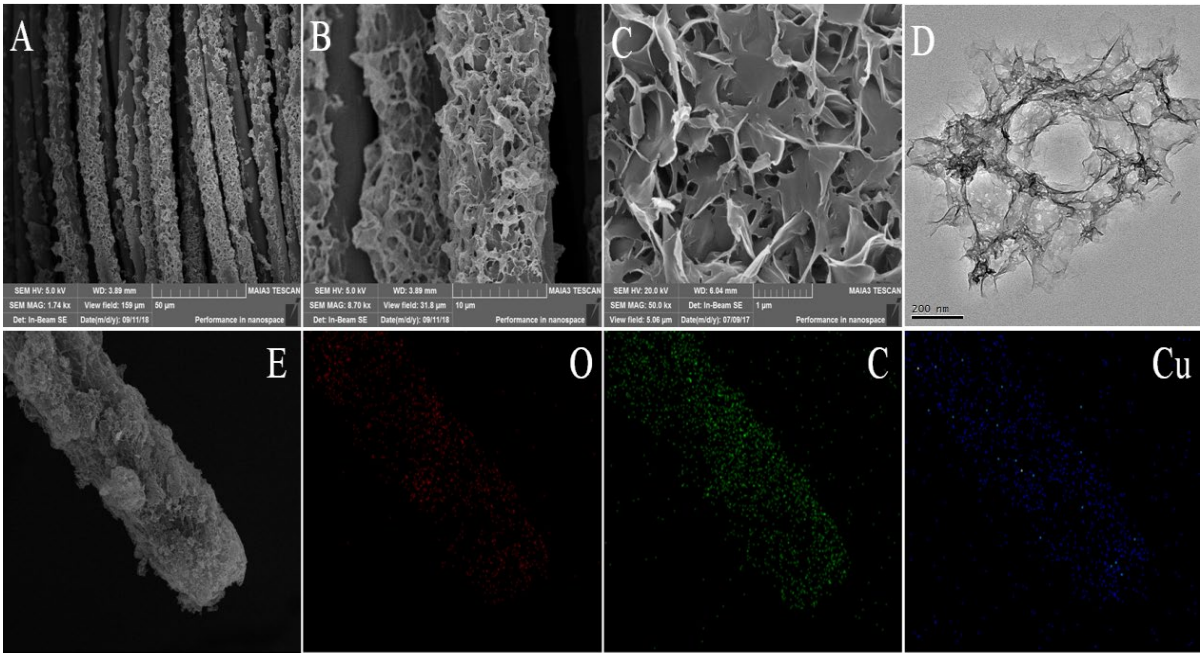

Fig. 1 (A and B) SEM images of MOF-74(Cu) NS-CC; (C) SEM image of MOF-74(Cu) NS; (D) TEM image of MOF-74(Cu) NS; (E) EDS mapping images of MOF-74(Cu) NS-CC.

two binding energies of Cu 2p3/2 (the Cu in MOF-74 (Cu) NS), 935.4 eV and 955.0 eV, which are in accord with $Cu(NO_3)_2$. In addition, in the binding energy range of 940-963 eV, a shake-up satellite peak was observed, which may further confirm that the copper exists as Cu^{2+} ions [33,34]. For pure Cu^{2+} ions, the Cu 2p3/2 binding energy is 935.2 eV. However, for the Cu^{2+} ions in MOF-74 (Cu) NS, the binding energy is shifted to higher energy. This may indicate a charge transfer from Cu^{2+} to the organic ligand [35]. The O1s spectra shows two main oxygen species in O1s spectra including 531.56 eV that is due to the C=O bond and 533.30 eV that derives from the contribution of C–OH/C–O–OH [36]. Four peaks were fitted from C1s spectra as shown in Fig. S2. The 288.6 eV is assigned to be the sp2-bonded carbon in the carboxylate group (O-C=O). The peaks emitted at 286.3 eV and 284.8 eV is assigned for the sp2-bonded carbon (C-C, C2), the peaks may be attributed from the contamination of carbon-containing matters [37]. The XRD patterns of MOF-74 (Cu) NS were shown in Fig. S4A and indicate that the existence of the characteristic signals at 2θ of 18.89°, 21.04° and 25.08° marked by their indices (202), (002) and (200), respectively. These diffraction peaks were found matched well with the MOF-74 (Cu) reported previously [38]. The results also indicate that MOF-74 (Cu) NS was well crystallized. In addition, from the FTIR spectra of MOF-74(Cu) NS shown in Fig. S3B, the asymmetric stretching of carboxylate group in DHTP appeared at 1524 and 1623 cm^{-1} while the symmetric stretching of the carboxylate groups in DHTP appeared at 1385

cm^{-1}. Several bands observed in 1025 and 800 cm^{-1} are assigned to the out-of-plane vibrations of DHTP [39]. The porous property of MOF-74(Cu) NS was shown in Fig. S3C. The BET surface area of MOF-74(Cu) NS was estimated to be 91.85 $m^2 \cdot g^{-1}$ and the total pore volume was 0.5507 $cm^3 \cdot g^{-1}$. From literature, it was generally reported that the BET surface area of 2D-MOF was about 100 $m^2\ g^{-1}$ or less. The relatively low BET surface area observed may be due to the low porosity in certain single-/multi-layer of the 2D-MOF structure [11,15,21]. Nonetheless, these characterization results support evidently the in-situ formation of MOF-74(Cu) NS on carbon cloth.

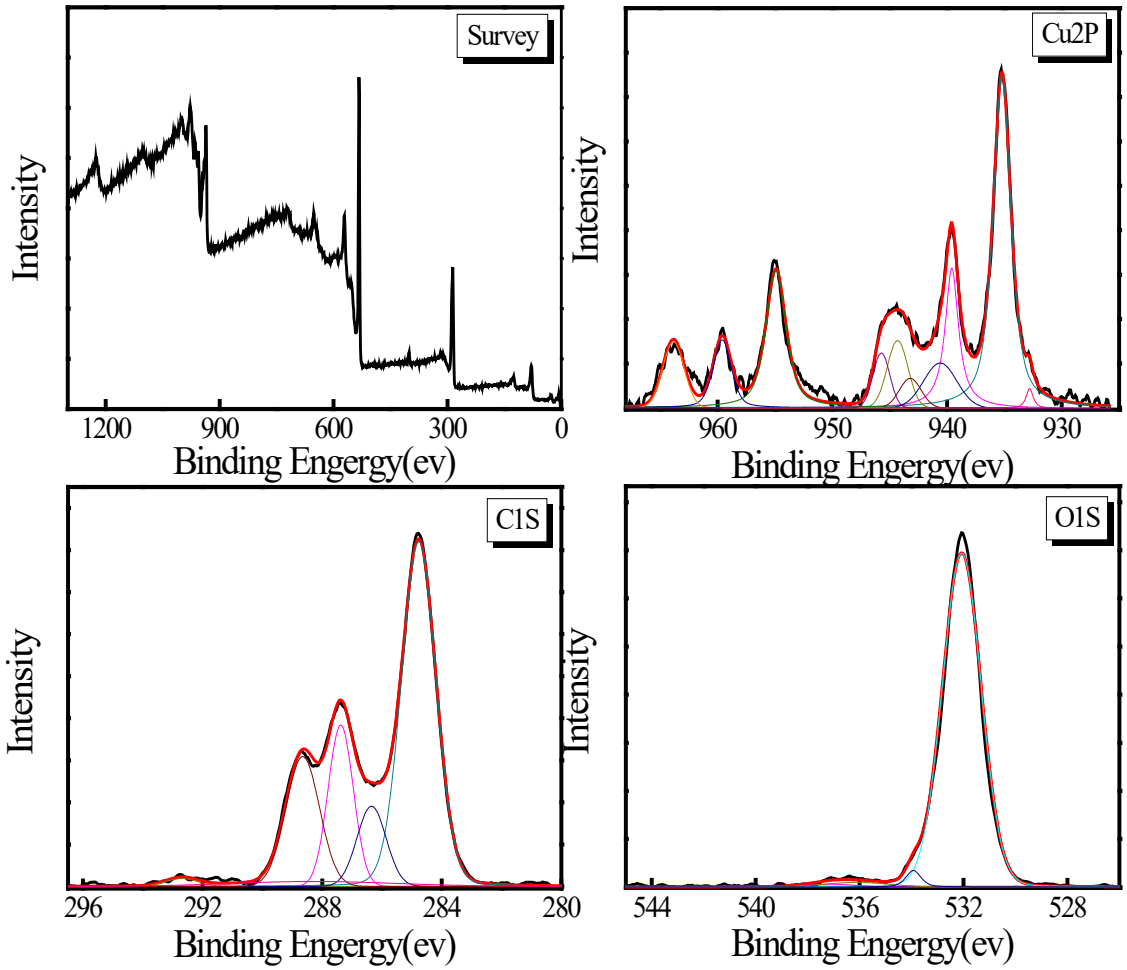

Fig. 2 The XPS spectra of MOF-74(Cu) NS. The survey of Cu 2p, C 1s and the O 1s spectra

3.2 The working mechanism of the proposed electrocatalytic biosensor based on MOF-74(Cu) NS-CC

A facile protocol to assemble the new MOF-74(Cu) NS-based electrocatalytic biosensor for the detection of glucose was showed in Scheme 1. The sensing system was developed with respect to the electrocatalytic activity of MOF-74(Cu) NS to catalyze the oxidation of glucose

to gluconate under alkaline conditions. In this sensing system, glucose was oxidized by the Cu^{3+} species, which were produced *in-situ* via the electrochemical oxidation of Cu^{2+} species under alkaline conditions [40]. The redox process could be detected by electrochemical workstation, in which the oxidation peak for glucose was observed at 0.55 V (vs Ag/AgCl). The higher the concentration of glucose present in the solution, the higher the oxidation current can be observed. When the electrocatalyst (MOF-74(Cu) NS) was *in-situ* deposited onto carbon cloth, the electrode (MOF-74(Cu) NS-CC) is able to provide a much better conductivity and electrocatalytic performance than MOF-74(Cu) NS-GCE. In addition, MOF-74(Cu) NS-CC is able to make the sensing process more convenient than that with the modified-GCE electrode because our new sensing system does not require additional electrode modification process such as calcinations.

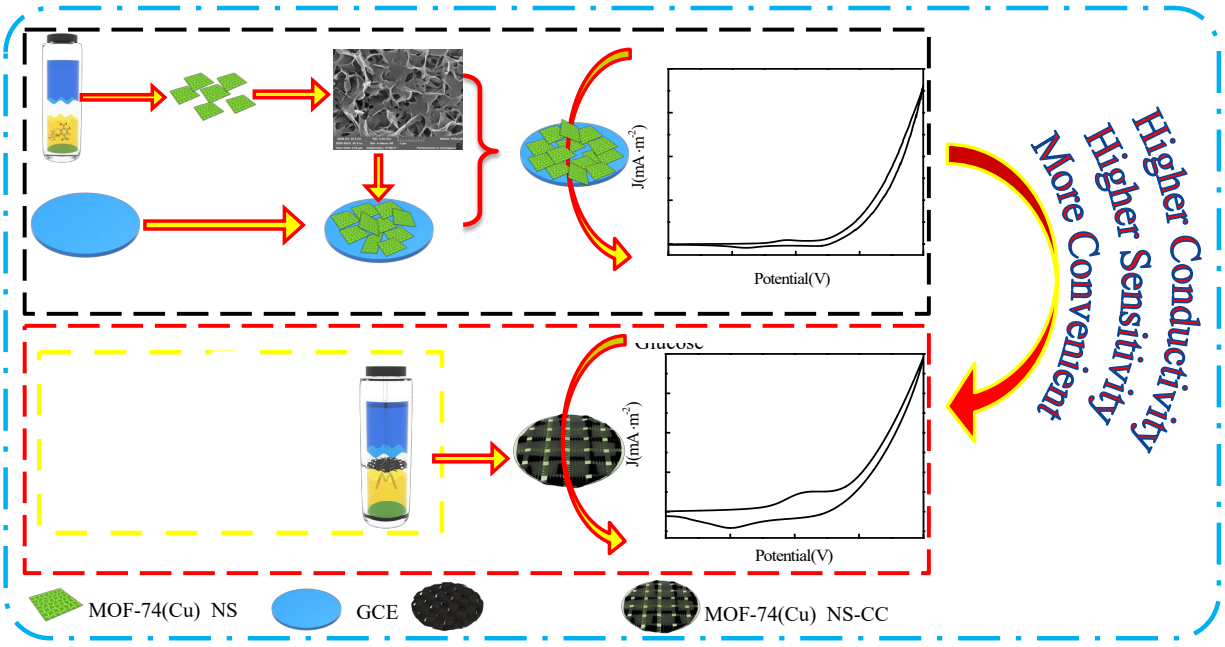

Scheme 1. A schematic diagram for the MOF-74(Cu) NS-CC electrocatalytic biosensors for the determination of glucose.

3.3 Electrochemical characterization of MOF-74(Cu) NS-CC for glucose detection

Electrochemical impedance spectroscopy (EIS) is widely used to study the characteristics of electrodes. As shown in Fig. 4A, the bare carbon cloth (CC) exhibited very low resistance while MOF-74(Cu) NS-CC has higher resistance compared to the bare CC. The result indicates that MOF-74(Cu) NS was successfully grown onto the CC surface. The MOF-

74(Cu) NS was also deposited onto GCE with nafion for comparison. The MOF-74(Cu) NS-GCE exhibited the highest resistance because the existence of nafion in the composite further reduced the conductivity of MOF-74(Cu) NS. The high resistance observed for MOF-74(Cu) NS-GCE also supports that MOF-74(Cu) NS was successfully immobilized onto the GCE surface [41].

The feasibility of direct use MOF-74(Cu) NS-CC as an electrosensor for glucose determination was investigated in a 0.1 M NaOH aqueous solution with or without glucose. As shown in Fig. 4B, upon the addition of glucose, a clear oxidation current with the peak potential at 0.55 V (vs Ag/AgCl) was observed, which indicated that MOF-74(Cu) NS is active to catalyze the oxidation of glucose (Glu). The electrochemical response of MOF-74(Cu) NS-CC towards Glu (1 mM) in the range of pH 9-14 was also investigated. As shown in Fig. 4C, there was no obvious glucose oxidation peak found under pH 9-12 because no Cu^{3+} species was produced to oxidize glucose under these pH conditions. As increasing the pH to 13 or 14, the Cu^{2+} ions of MOF-74(Cu) NS-CC were oxidized to Cu^{3+} upon the current was applied. The results support that the electrochemically generated Cu^{3+} species are able to oxidize glucose to gluconate efficiently at pH 13-14 and a current peak at 0.55 V (vs Ag/AgCl) was observed. It was found that the electrochemical response of MOF-74(Cu) NS-CC towards 1 mM Glu at pH 13 was the best condition. The corresponding catalytic mechanism is illustrated by the following equations:

(1) 2MOF-74(Cu) NS-Cu(II) → 2MOF-74(Cu) NS-Cu(III) + e^-

(2) 2MOF-74(Cu) NS-Cu(III)+Glucose → Gluconolacton+2MOF-74(Cu) NS-Cu(II)+H_2O

(3) Gluconolacton+H_2O → H^+ + Gluconate

In order to further investigate the mechanism of the electrosensor, the cyclic voltammogram (CV) curves of MOF-74(Cu) NS-CC in 25 mM PBS (pH 7.0) were obtained. As shown in Fig. 4D, when it was scan from 0 to 0.7 V (vs Ag/AgCl), the Cu(II) in MOF-74(Cu) NS was oxidized to Cu(III) and an oxidation peak was recorded at 0.55 V (vs Ag/AgCl). The Cu(III) species is active catalyst to oxidize the glucose to gluconate in alkaline solution and the Cu(III) species was reduced to Cu(II) during the reaction. The corresponding reduction

signal was recorded at 0.4 V when it was scanned from 0.7 to 0 V (vs Ag/AgCl). Moreover, the electron transfer number was calculated according to the following equation [42]:

(4) $|Ep-Ep/2|=2.20RT/nF$

Where Ep is the peak potential, Ep/2 is the half peak potential, F is the Faraday constant (96485 C mol^{-1}), R is a universal gas constant (8.314 J K^{-1} mol^{-1}), T is the Kelvin temperature (298 K). As shown in Fig. 4D, the values of |Ep-Ep/2| for the oxidation peak and reduction peak were determined to be 55.8 mV and 56 mV, respectively. Thus according to Eq. (4), the values of n for both oxidation and reduction were calculated to be 1.01 and 1.008, respectively. The results indicate that it is a single electron transfer system when applying MOF-74(Cu) NS-CC as working electrode.

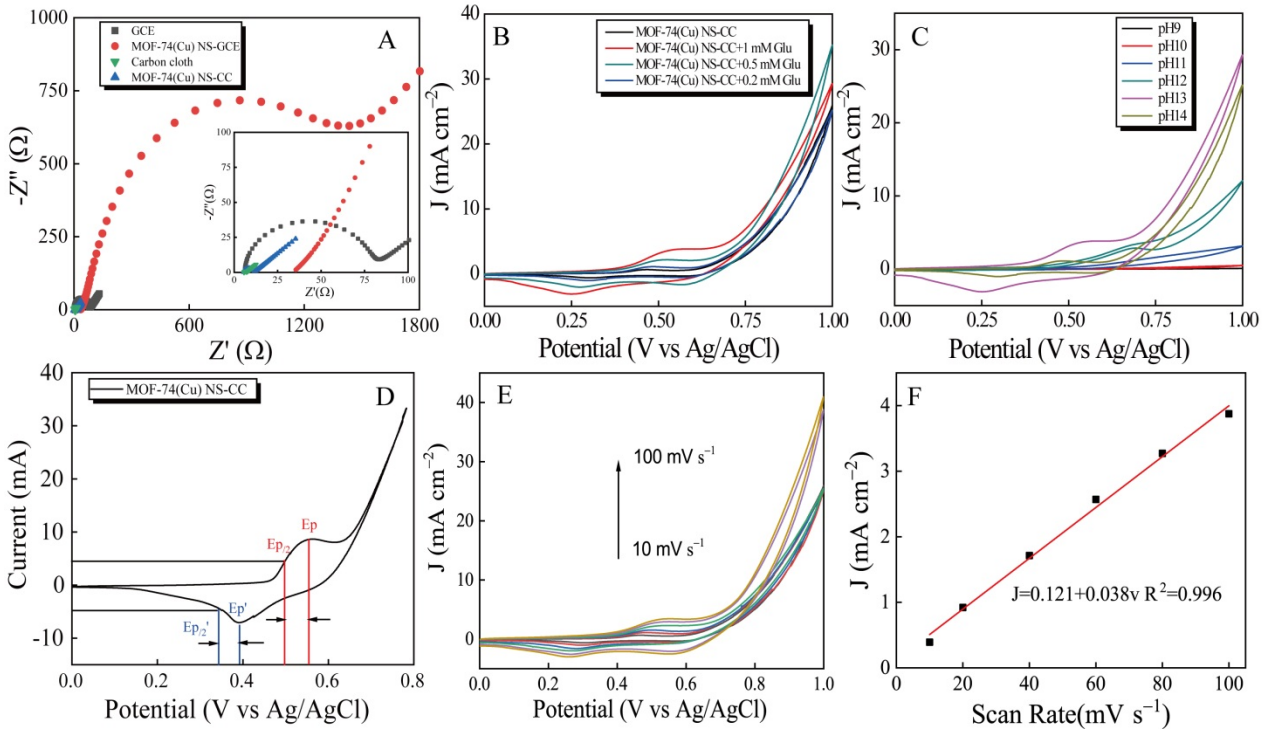

Fig.4 (A) Nyquist diagrams of 0.1 mM NaOH at GCE, MOF-74(Cu) NS-GCE, carbon cloth and MOF-74(Cu) NS-CC; (B) Feasibility analysis of the electrocatalytic sensor to detect Glu with MOF-74(Cu) NS-CC; (C) The CV spectra of MOF-74 (Cu) NS-CC in different pH; (D) CV curve of MOF-74(Cu) NS-CC in 25 mM PBS (pH 7.0); (E) The CV spectra of MOF-74 (Cu) NS-CC with 1 mM glucose in different scan rate; (F) The plot of the relationship between square root of scan rates and the current density.

The cyclic voltammograms of using MOF-74(Cu) NS-CC as the working electrode in a NaOH aqueous solution (0.1 M) containing glucose (1 mM) were obtained at different scan

rates. As shown in Fig. 4E and F, the current density increases with the increasing of scan rates from 10 to 100 mV s^{-1}. A linear relationship between the peak current densities and the square root of scan rates was established (Fig. 4F). The results may imply that the glucose oxidation occurred on MOF-74(Cu) NS-CC electrode is probably a diffusion controlled process [43].

3.3 Calibration curve for the determination of glucose

Fig. 5A shows the current density responses of MOF-74 (Cu) NS-CC after the reaction with glucose at different concentrations. The current density increased gradually with respect to the increasing concentration of glucose in the range of 1.0 to 1000 μM. Moreover, Fig. 5B shows a good linear relationship between the current density and glucose concentrations. The linear equations were established as follows:

$$\Delta J = 3.39[C_{(Glu)}] + 240.0 \quad R^2=0.997 \quad ([C_{(Glu)}] = 1\text{-}80\ \mu M)$$

$$\Delta J = 3.81[C_{(Glu)}] + 190.6 \quad R^2=0.997 \quad ([C_{(Glu)}] = 100\text{-}1000\ \mu M)$$

The limit of detection (LOD) was 0.41 μM (S/N=3) and the response sensitivity calculated was 3.39 mA mM^{-1} cm^{-2} when the glucose concentration was in the range of 1-80 μM and 3.81 mA mM^{-1} cm^{-2} for the 100-1000 μM.

We further investigated the performance of MOF-74(Cu) NS-GCE in the determination for glucose for comparison. As show in Fig. 5C, the current density increased gradually with respect to the concentration of glucose increasing from 5.0 to 100 μM. The linear equation obtained was $\Delta J = 2.25[C_{(Glu)}](\mu M) - 1.7$ with a $R^2 = 0.997$. The LOD was 1.9 μM (S/N=3). The response sensitivity was calculated to be 2.25 mA mM^{-1} cm^{-2}, which is significantly lower than that of MOF-74 (Cu) NS-CC. The results reveal that MOF-74(Cu) NS-CC exhibits better performance in the determination of glucose, which may be attributed to its high conductivity. The performance of this electrosensor was also compared with other nanomaterials-based sensors reported recently. As listed in Table 1, we found that MOF-74 (Cu) NS-CC exhibits higher sensitivity, lower detection limit and wider linear range than most reported sensing systems in the detection of glucose. For the palladium based nanomaterials such as Pd/PEDOT [44], PdFe alloy [45] and Pd–Ni alloy [46] do not exhibit better

performance than the present study. Moreover, palladium as noble metal presents some drawbacks such as high cost and low abundance. MOF-74(Cu) NS is the copper-based materials, which is the abundant metal and thus has more advantage than the palladium-based materials. Another electrocatalytic glucose sensor based on CuO-NA-GCE, which is constructed by calcination of Cu-MOF [47], gave a slightly better LOD (0.15 μM) than MOF-74 (Cu) NS-CC (0.41 μM). However, MOF-74 (Cu) NS-CC biosensor can be *in-situ* fabricated by one-step synthesis and also can be utilized directly as the working electrode without modification process required.

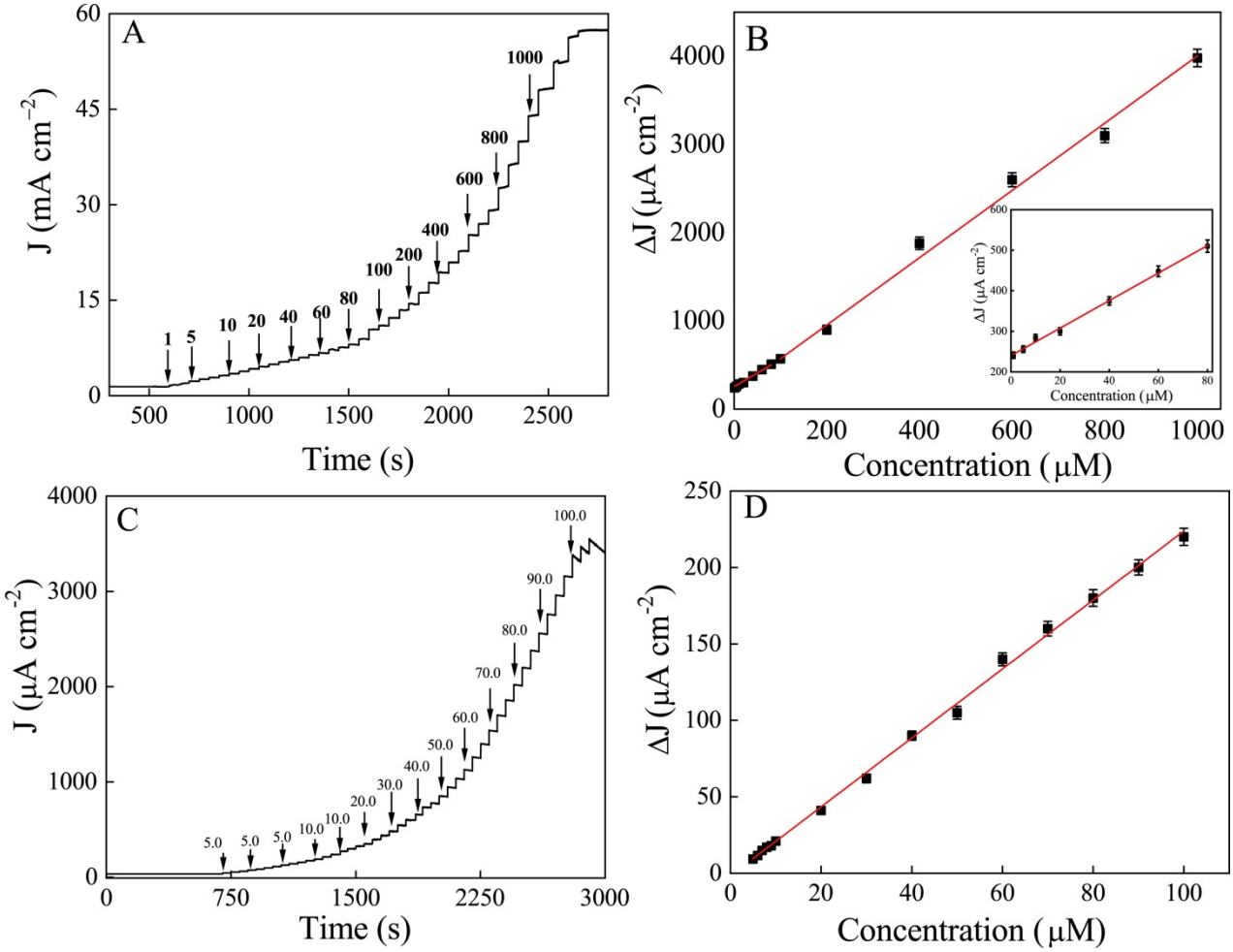

Fig.5 (A) Amperometric sensing and the corresponding calibration curve of Glu by successive addition of Glu at MOF-74 (Cu) NS-CC at 0.55 V (vs Ag/AgCl) in 0.1 M NaOH solution; (B) The corresponding calibration curve of Glu by successive addition of Glu at MOF-74 (Cu) NS-CC, the insert plot was the fitting curve in the range of 1-80 μM; (C) Amperometric sensing and the corresponding calibration curve of Glu by successive addition of Glu at MOF-74 (Cu) NS-GCE at 0.55 V (vs Ag/AgCl) in 0.1 M NaOH solution;

(D) The corresponding calibration curve of Glu by the successive addition of Glu at MOF-74 (Cu) NS-GCE.

<<Preferred location for Table 1>>

3.4 The study of selectivity, reproducibility and stability of the sensor

To avoid the interference responses for nonenzymatic sensors is one of the great challenges in analysis of glucose in human serum samples. The primary interferents such as lactose (Lac), fructose (Fru), glyphosate (Gly), hydroquinone (HQ) and catechol (CTH) exhibit a comparable electroactive activity to glucose. In addition, ascorbic acid (AA) calcium ion (Ca^{2+}), magnesium ions (Mg^{2+}) and uric acid (UA) are also present in the blood serum samples and all these interferents may affect the performance of sensors [43]. Therefore, to evaluate the anti-interference performance of our new biosensor towards these potential interfering species is essential. Fig. 6A exhibited the amperometric responses of the MOF-74(Cu) NS-CC at 0.55 V in 0.1 M NaOH aqueous solution after the addition of 50.0 μM Glu, 5.0 mM AA, 10 mg mL^{-1} Lac, 10 mM Ca^{2+}, 10 mM Mg^{2+}, 5.0 mM Fru, 5.0 mM UA, 0.5 mM Gly, 0.5 mM HQ and 0.5 mM CTH successively. The results clearly showed that MOF-74(Cu) NS-CC gives response selectively for Glu only, while the response for the interferents examined was weak and negligible. The previous work reported that Gly, HQ and CTH could be oxidized with electrocatalysts to produce current response under either weak acid and weak base conditions [48,49]. However, the sensing condition of MOF-74(Cu) NS-CC was conducted in an alkaline condition (pH 13-14), therefore, this electrocatalytic biosensor showed no response to Gly, HQ and CTH. Moreover, the current density can increased again with second addition of glucose (50 μM) as shown in Fig. 6A and B. The results may indicate that MOF-74(Cu) NS-CC biosensor has very high selectivity towards glucose.

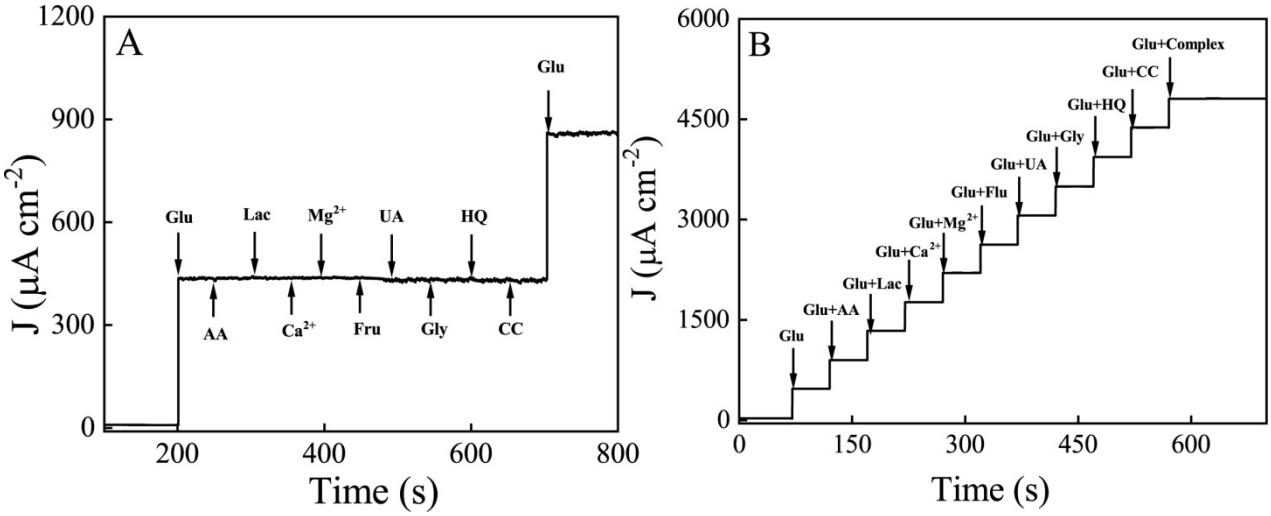

Fig.6 (A) Selectivity and (B) anti-interferential tests of the proposed sensors. Glu (50 μM), AA (1 mM), Lac (10 mg mL^{-1}), Ca^{2+} (10 mM), Mg^{2+} (10 mM), Fru (1 mM), UA (10 mM), Gly (0.5 mM), HQ (0.5 mM) and CTH (0.5 mM).

The manufacturing reproducibility was assessed by comparing the current generated from proposed electrocatalytic biosensors fabricated independently in a 0.1 M NaOH aqueous solution with 50 μM glucose for six times. The relative standard deviation (RSD) obtained is 5.6%, indicating that our synthetic protocol has very good reproducibility. In addition, to demonstrate the stability and long-term stability of the biosensor, MOF-74(Cu) NS-CC electrode was freshly fabricated and was tested in a 0.1 M NaOH aqueous solution with 50 μM glucose and then was stored at ambient conditions for 30 days. After that, the biosensor was re-assessed under the same conditions and only 6% of the current density was decreased compared to its original as shown in Fig. S4. The results show that the electrocatalytic biosensor has high stability.

3.5 Determination of glucose in serum samples

To verify the feasibility of using MOF-74(Cu) NS-CC for routine and practical analysis, the sensor was utilized to detect glucose in human serum. The test procedures and conditions were briefly described as follows. Three human serum samples (0.1 mL each), which were obtained from Xiamen Hospital of Traditional Chinese Medicine, were diluted with 9.9 mL of 0.1 M NaOH aqueous solution independently. The concentrations of glucose determined in these samples were 8.12 mM, 4.93 mM and 5.47 mM, respectively, which were very

comparable with the sample concentrations given by the hospital (Table 2). In addition, the recoveries were examined using the method of standard addition. Three serum samples given by the hospital~~, without further dilution,~~ were spiked with standard solution of glucose (1.0 mM, 2.0 mM and 4.0 mM, respectively). The spiked concentration was chosen based on the normal concentration of glucose in blood, which is in the range of 80-120 mg dL^{-1} (4.4-6.6 mM) [50]. The recoveries observed with MOF-74(Cu) NS-CC biosensor were in the range of 96-104% (Table 2). These results indicate that the present protocol is feasible and reliable to fabricate biosensors for the determination of glucose from human serum samples.

<<Preferred location for Table 2>>

Conclusion

In conclusion, a new MOF-74(Cu) NS-CC based electrocatalytic biosensor with excellent sensing performance was developed through one-step *in-situ* formation of MOF-74(Cu) NS onto the surface of carbon cloth in a multi-layer solution. Compared with the use of a glassy carbon electrode modified with MOF-74(Cu) NS as a working electrode for the determination of glucose, MOF-74(Cu) NS-CC exhibited much higher conductivity and higher sensitivity. More importantly, the method of *in-situ* deposition MOF-74(Cu) NS onto a conductive substrate with no calcination process required is more convenient than that of using glassy carbon electrode modification. The MOF-74(Cu) NS-CC biosensor was also demonstrated in the determination of glucose directly from real human serum samples. The results showed that the biosensor is accurate and reliable. The present study also demonstrates the potential application of two-dimensional metal organic frameworks to fabricate electrochemical sensors *in-situ* for analytical applications.

Acknowledgments

The authors gratefully acknowledged the financial support of STS Key Project of Fujian Province (2017T3007), Nature Sciences Funding of Fujian Province (2018J01682) and the Project of Quangang District Science and Technology Bureau (2019G01), and Nature Science Foundation of Guangdong Province (2019A1515011799).

Reference

1. Pang Y, Zang X, Li H, Liu J, Chang Q, Zhang S, Wang C, Wang Z (2020) Solid-phase microextraction of organophosphorous pesticides from food samples with a nitrogen-doped porous carbon derived from g-C3N4 templated MOF as the fiber coating. Journal of Hazardous Materials 384:121430

2. Li JT, Huang WZ, Wang MM, Xi SB, Meng JS, Zhao KN, Jin J, Xu WW, Wang ZY, Liu X, Chen Q, Xu LH, Liao XB, Jiang YL, Owusu KA, Jiang BL, Chen CX, Fan DNA, Zhou L, Mai LQ (2019) Low-Crystalline Bimetallic Metal-Organic Framework Electrocatalysts with Rich Active Sites for Oxygen Evolution. Acs Energy Letters 4:285-292

3. Fan WD, Wang X, Liu XP, Xu B, Zhang XR, Wang WJ, Wang XK, Wang YT, Dai FN, Yuan DQ, Sun DF (2019) Regulating C2H2 and CO2 Storage and Separation through Pore Environment Modification in a Microporous Ni-MOF. Acs Sustainable Chemistry & Engineering 7:2134-2140

4. Cabrera-Garcia A, Checa-Chavarria E, Rivero-Buceta E, Moreno V, Fernandez E, Botella P (2019) Amino modified metal-organic frameworks as pH-responsive nanoplatforms for safe delivery of camptothecin. Journal of Colloid and Interface Science 541:163-174

5. Lai H, Li G, Xu F, Zhang Z (2020) Metal–organic frameworks: opportunities and challenges for surface-enhanced Raman scattering–a review. Journal of Materials Chemistry C 8:2952-2963

6. Hu S, Ouyang W, Guo L, Lin Z, Jiang X, Qiu B, Chen G (2017) Facile synthesis of Fe3O4/g-C3N4/HKUST-1 composites as a novel biosensor platform for ochratoxin A. Biosensors and Bioelectronics 92:718-723

7. Song JY, He WT, Shen H, Zhou ZX, Li MQ, Su P, Yang Y (2019) Construction of multiple enzyme metal-organic frameworks biocatalyst via DNA scaffold: A promising strategy for enzyme encapsulation. Chemical Engineering Journal 363:174-182

8. Gkaniatsou E, Sicard C, Ricoux R, Benahmed L, Bourdreux F, Zhang Q, Serre C, Mahy JP, Steunou N (2018) Enzyme Encapsulation in Mesoporous Metal-Organic Frameworks for Selective Biodegradation of Harmful Dye Molecules. Angewandte Chemie-International Edition 57:16141-16146

9. Yi XR, He XB, Yin FX, Chen BH, Li GR, Yin HQ (2019) Co-CoO-Co3O4/N-doped carbon derived from metal-organic framework: The addition of carbon black for boosting oxygen electrocatalysis and Zn-Air battery. Electrochimica Acta 295:966-977

10. Mukherjee S, Cullen DA, Karakalos S, Liu KX, Zhang H, Zhao S, Xu H, More KL, Wang GF, Wu G (2018) Metal-organic framework- derived nitrogen-doped highly disordered carbon for electrochemical ammonia synthesis using N-2 and H2O in alkaline electrolytes. Nano Energy 48:217-226

11. Hu SS, Yan JJ, Huang XM, Guo LH, Lin ZY, Luo F, Qiu B, Wong KY, Chen GN (2018) A sensing platform for hypoxanthine detection based on amino-functionalized metal organic framework nanosheet with peroxidase mimic and fluorescence properties. Sensors and Actuators B-Chemical 267:312-319

12. Salunkhe RR, Kaneti YV, Kim J, Kim JH, Yamauchi Y (2016) Nanoarchitectures for Metal-Organic Framework-Derived Nanoporous Carbons toward Supercapacitor Applications. Accounts of Chemical Research 49:2796-2806

13. Zhong H, Ly KH, Wang M, Krupskaya Y, Han X, Zhang J, Zhang J, Kataev V, Büchner B, Weidinger IM (2019) A Phthalocyanine‐Based Layered Two‐Dimensional Conjugated Metal–Organic Framework as a Highly Efficient Electrocatalyst for the Oxygen Reduction Reaction. Angewandte Chemie 131:10787-10792

14. Xiao Q-Q, Liu D, Wei Y-L, Cui G-H (2019) A new multifunctional two-dimensional cobalt (II) metal–organic framework for electrochemical detection of hydrogen peroxide, luminescent sensing of metal ions, and photocatalysis. Polyhedron 158:342-351

15. Zhao M, Wang Y, Ma Q, Huang Y, Zhang X, Ping J, Zhang Z, Lu Q, Yu Y, Xu H (2015) Ultrathin 2D metal–organic framework nanosheets. Advanced Materials 27:7372-7378

16. Wang Q, Yang Y, Gao F, Ni J, Zhang Y, Lin Z (2016) Graphene oxide directed one-step synthesis of flowerlike graphene@ HKUST-1 for enzyme-free detection of hydrogen peroxide in biological samples. ACS applied materials &

interfaces 8:32477-32487
17. Yin D, Liu J, Bo X, Li M, Guo L (2017) Porphyrinic metal-organic framework/macroporous carbon composites for electrocatalytic applications. Electrochimica Acta 247:41-49
18. Chaudhari NK, Jin H, Kim B, Lee K (2017) Nanostructured materials on 3D nickel foam as electrocatalysts for water splitting. Nanoscale 9:12231-12247
19. Zha Q, Li M, Liu Z, Ni Y (2020) Hierarchical Co, Fe-MOF-74/Co/Carbon Cloth Hybrid Electrode: Simple Construction and Enhanced Catalytic Performance in Full Water Splitting. ACS Sustainable Chemistry & Engineering 8:12025-12035
20. Zhang L, Zhang Y, Huang S, Yuan Y, Li H, Jin Z, Wu J, Liao Q, Hu L, Lu J (2018) Co3O4/Ni-based MOFs on carbon cloth for flexible alkaline battery-supercapacitor hybrid devices and near-infrared photocatalytic hydrogen evolution. Electrochimica Acta 281:189-197
21. Hu S, Zhu L, Lam CW, Guo L, Lin Z, Qiu B, Wong KY, Chen G, Liu Z (2019) Fluorometric determination of the activity of inorganic pyrophosphatase and its inhibitors by exploiting the peroxidase mimicking properties of a two-dimensional metal organic framework. Microchimica Acta 186:190
22. Chang J, Li H, Hou T, Duan W, Li F (2018) Paper-based fluorescent sensor via aggregation induced emission fluorogen for facile and sensitive visual detection of hydrogen peroxide and glucose. Biosensors and Bioelectronics 104:152-157
23. Gu C, Gai P, Hou T, Li H, Xue C, Li F (2017) Enzymatic fuel cell-based self-powered homogeneous immunosensing platform via target-induced glucose release: an appealing alternative strategy for turn-on melamine assay. ACS applied materials & interfaces 9:35721-35728
24. Neto SA, Almeida TS, Palma LM, Minteer SD, Andrade ARD (2014) Hybrid nanocatalysts containing enzymes and metallic nanoparticles for ethanol/O 2 biofuel cell. Journal of Power Sources 259:25-32
25. Mahmoud MA, O'Neil D, El-Sayed MA Hollowand Solid Metallic Nanoparticles in Sensingand in Nanocatalysis. Chemistry of Materials 26:44-58
26. Zhao L, Thomas JP, Heinig NF, Abd-Ellah M, Wang X, Leung KT (2014) Au–Pt alloy nanocatalysts for electro-oxidation of methanol and their application for fast-response non-enzymatic alcohol sensing. Journal of Materials Chemistry C 2:2707-2714
27. Wu XF, Bao CC, Niu QQ, Lu WB (2019) A novel method to construct a 3D FeWO4 microsphere-array electrode as a non-enzymatic glucose sensor. Nanotechnology 30:165501
28. Lu WB, Wu XF (2018) Ni-MOF nanosheet arrays: efficient non-noble-metal electrocatalysts for non-enzymatic monosaccharide sensing. New Journal of Chemistry 42:3180-3183
29. Shahhoseini L, Mohammadi R, Ghanbari B, Shahrokhian S (2019) Ni(II) 1D-coordination polymer/C-60-modified glassy carbon electrode as a highly sensitive non-enzymatic glucose electrochemical sensor. Applied Surface Science 478:361-372
30. Darabdhara G, Bordoloi J, Manna P, Das MR (2019) Biocompatible bimetallic Au-Ni doped graphitic carbon nitride sheets: A novel peroxidase-mimicking artificial enzyme for rapid and highly sensitive colorimetric detection of glucose. Sensors and Actuators B-Chemical 285:277-290
31. Dong SY, Zhang DD, Cui H, Huang TL (2019) ZnO/porous carbon composite from a mixed-ligand MOF for ultrasensitive electrochemical immunosensing of C-reactive protein. Sensors and Actuators B-Chemical 284:354-361
32. Li Y, Dai H, Zhang Q, Zhang S, Chen S, Hong Z, Lin Y (2016) In situ generation of electron acceptor to amplify the photoelectrochemical signal from poly (dopamine)-sensitized TiO 2 signal crystal for immunoassay. Journal of Materials Chemistry B 4:2591-2597
33. Wan Y, Ma JX, Wang Z, Zhou W, Kaliaguine S (2005) On the mechanism of selective catalytic reduction of NO by propylene over Cu-Al-MCM-41. Applied Catalysis B-Environmental 59:235-242
34. Huang J, Wang S, Guo X, Wang D, Zhu B, Wu S (2008) The preparation and catalytic behavior of CuO/TixSn1− xO2 catalysts for low-temperature carbon monoxide oxidation. Catalysis Communications 9:2131-2135

35. Chen XY, Chen C, Zhang ZJ, Xie DH (2013) Gelatin-derived nitrogen-doped porous carbon via a dual-template carbonization method for high performance supercapacitors. Journal of Materials Chemistry A 1:10903-10911
36. Qin J, Wang S, Ren H, Hou Y, Wang X (2015) Photocatalytic reduction of CO2 by graphitic carbon nitride polymers derived from urea and barbituric acid. Applied Catalysis B: Environmental 179:1-8
37. Rong M, Lin L, Song X, Zhao T, Zhong Y, Yan J, Wang Y, Chen X (2015) A label-free fluorescence sensing approach for selective and sensitive detection of 2, 4, 6-trinitrophenol (TNP) in aqueous solution using graphitic carbon nitride nanosheets. Analytical chemistry 87:1288-1296
38. Ruano D, Díaz‐García M, Alfayate A, Sánchez‐Sánchez M (2015) Nanocrystalline M‐MOF‐74 as Heterogeneous Catalysts in the Oxidation of Cyclohexene: Correlation of the Activity and Redox Potential. ChemCatChem 7:674-681
39. Dang GH, Lam HQ, Nguyen AT, Le DT, Truong T, Phan NT (2016) Synthesis of indolizines through aldehyde–amine–alkyne couplings using metal-organic framework Cu-MOF-74 as an efficient heterogeneous catalyst. Journal of catalysis 337:167-176
40. Zhang Y, Su L, Manuzzi D, de los Monteros HVE, Jia W, Huo D, Hou C, Lei Y (2012) Ultrasensitive and selective non-enzymatic glucose detection using copper nanowires. Biosensors and Bioelectronics 31:426-432
41. Kang X, Mai Z, Zou X, Cai P, Mo J (2007) A sensitive nonenzymatic glucose sensor in alkaline media with a copper nanocluster/multiwall carbon nanotube-modified glassy carbon electrode. Analytical biochemistry 363:143-150
42. Nenkova R, Wu J, Zhang Y, Godjevargova T (2013) Influence of different nanozeolite particles on the sensitivity of a glucose biosensor. Analytical biochemistry 439:65-72
43. Chen T, Liu D, Lu W, Wang K, Du G, Asiri AM, Sun X (2016) Three-dimensional Ni2P nanoarray: an efficient catalyst electrode for sensitive and selective nonenzymatic glucose sensing with high specificity. Analytical chemistry 88:7885-7889
44. Hosseini H, Rezaei SJT, Rahmani P, Sharifi R, Nabid MR, Bagheri A (2014) Nonenzymatic glucose and hydrogen peroxide sensors based on catalytic properties of palladium nanoparticles/poly(3,4-ethylenedioxythiophene) nanofibers. Sensors & Actuators B Chemical 195:85-91
45. Wang J, Wang Z, Zhao D, Xu C (2014) Facile fabrication of nanoporous PdFe alloy for nonenzymatic electrochemical sensing of hydrogen peroxide and glucose. Analytica Chimica Acta 832:34-43
46. Zhao D, Xu C (2015) A nanoporous palladium-nickel alloy with high sensing performance towards hydrogen peroxide and glucose. Journal of Colloid & Interface Science 447:50-57
47. Luo Y, Wang Q, Li J, Xu F, Sun L, Bu Y, Zou Y, Kraatz H-B, Rosei F (2020) Tunable hierarchical surfaces of CuO derived from metal–organic frameworks for non-enzymatic glucose sensing. Inorganic Chemistry Frontiers 7:1512-1525
48. Gu C, Wang Q, Zhang L, Yang P, Xie Y, Fei J (2020) Ultrasensitive non-enzymatic pesticide electrochemical sensor based on HKUST-1-derived copper oxide@ mesoporous carbon composite. Sensors and Actuators B: Chemical 305:127478
49. Alshahrani LA, Miao L, Zhang Y, Cheng S, Sathishkumar P, Saravanakumar B, Nan J, Gu FL (2019) 3D-flower-like copper sulfide nanoflake-decorated carbon nanofragments-modified glassy carbon electrodes for simultaneous electrocatalytic sensing of co-existing hydroquinone and catechol. Sensors 19:2289
50. Wang J (2008) Electrochemical glucose biosensors. Chemical reviews 108:814-825
51. Liu M, Ru L, Wei C (2013) Graphene wrapped Cu 2 O nanocubes: Non-enzymatic electrochemical sensors for the detection of glucose and hydrogen peroxide with enhanced stability. Biosensors & Bioelectronics 45:206-212
52. Li Y, Zhong Y, Zhang Y, Weng W, Li S (2015) Carbon quantum dots/octahedral Cu2O nanocomposites for non-enzymatic glucose and hydrogen peroxide amperometric sensor. Sensors and Actuators B: Chemical 206:735-743
53. Gao W, Tjiu WW, Wei J, Liu T (2014) Highly sensitive nonenzymatic glucose and H2O2 sensor based on Ni (OH) 2/electroreduced graphene oxide− Multiwalled carbon nanotube film modified glass carbon electrode. Talanta 120:484-490

Table 1. Comparative characteristics of the as-prepared biosensor and some other sensors for the determination of glucose.

Electrode material	Oxidation potential	Linear range /mM	LOD /μM	Response sensitivity / $mA \cdot mM^{-1} \cdot cm^{-2}$	Ref
Pd/PEDOT	~0.1 V (Ag/AgCl)	0.04-9	1.6	-	[44]
PdFe alloy	0.35 V (RHE)	1-32	1.6	0.0027	[45]
Graphene wrapped Cu_2O	0.8 V (SCE)	0.3-3.3	3.3	-	[51]
Pd–Ni alloy	1.0 V (SCE)	0.05-1.0	2.1	0.75	[46]
CQDts/Cu_2O	0.6 V (SCE)	0.02-4.3	8.4	0.13	[52]
$Ni(OH)_2$/GO-MWCNT	0.54 V (SCE)	0.01-1.5	2.7	2.04	[53]
CuO-350-NA-GCE	0.55 V (Ag/AgCl)	0-6.5	0.15	1.80	[47]
MOF-74(Cu) NS-GCE	0.55 V (Ag/AgCl)	0.005-0.1	1.9	2.25	This work
MOF-74(Cu) NS-CC	0.55 V (Ag/AgCl)	0.001-1.0	0.41	3.75	This work

Table 2. Determination of glucose in human serum by electrocatalytic biosensor.

Sample	Detected (mM)	Clinical results from Hospital (mM)	Spiked (mM)	Total found (mM)	Recovery	RSD
1	4.95	4.93	1.0	5.89	96%	5.2%
			2.0	6.91	99%	4.1%
			4.0	9.01	102%	4.4%
2	5.39	5.47	1.0	6.51	104%	4.7%
			2.0	7.48	100.5%	4.5%
			4.0	9.56	101.7%	5.0%
3	8.07	8.12	1.0	8.97	97.0%	5.1%
			2.0	10.08	98.0%	5.6%
			4.0	12.21	102.5%	4.7%

Supporting Information

In-situ deposition of MOF-74(Cu) nanosheet arrays onto carbon cloth to fabricate a sensitive and selective electrocatalytic biosensor and its application in the determination of glucose in human serum

Shuisheng Hu[1,a,b], Yuxia Lin[1,a] , Jing Teng*[,c], Wing-Leung Wong*[,b], Bin Qiu*[,a]

[a] Ministry of Education Key Laboratory for Analytical Science of Food Safety and Biology, Fujian Provincial Key Laboratory of Analysis and Detection for Food Safety, Fuzhou University, Fuzhou, Fujian, 350108, P. R. China.

[b] Department of Applied Biology and Chemical Technology and State Key Laboratory of Chemical Biology and Drug Discovery, The Hong Kong Polytechnic University, Hunghom, Kowloon, Hong Kong, P. R. China.

[c] Department of Laboratory, Xiamen Hospital of Traditional Chinese Medicine, Xiamen Hospital, Beijing University of Chinese Medicine, Xiamen TCM Hospital Affiliated to Fujian University of Traditional Chinese Medicine.

Corresponding author:

E-mail: summer328cn@163.com (Bin Qiu);

E-mail: tengjing1108@163.com (Jing Teng).

E-mail: wing.leung.wong@polyu.edu.hk (Wing-Leung Wong);

[1] These authors contributed equally to this work

Tel: 86-591-22866135

Caption

1. Preparation of MOF-74(Cu) NS;

2. Fabrication of MOF-74(Cu) NS-GCE the working electrode;

3. Characterization of MOF-74(Cu) NS and MOF-74(Cu) NS-CC;

4. The assay to detect glucose by MOF-74(Cu) NS-CC;

Fig. S1 Picture showing the spatial arrangement of different liquid layers during the synthesis of MOF-74(Cu) NS-CC;

Fig. S2 AFM image of MOF-74(Cu) NS;

Fig. S3 XRD patterns, FTIR spectra and N_2 adsorption–desorption isotherms of MOF-74(Cu) NS;
(A) XRD patterns for MOF-74(Cu) NS;
(B) FTIR spectra for MOF-74(Cu) NS;
(C) N_2 adsorption-desorption isotherms for MOF-74(Cu) NS.

Fig. S4 Long-term stability of the MOF-74(Cu) NS-CC based electrocatalytic sensor. MOF-74(Cu) NS-CC was stored at ambient conditions over 30 days. Data recorded at 0.1 M NaOH with addition of 50 μM glucose at 0.55 V vs Ag/AgCl.

1. Preparation of MOF-74(Cu) NS

MOF-74(Cu) NS was synthesized in a glass tube similar to previous report[1]. The set up was shown in Fig. S1, which has three layers of solutions. A mixed solution of CH_3CN (3 mL) and DMF (6 mL) containing DHTP (60 mg) and injected into a glass tube as the bottom layer. On top of this solution, a solution mixed with CH_3CN (3 mL) and DMF (3 mL) was slowly added as the middle layer. Finally, a solution containing $Cu(NO_3)_2 \cdot 3H_2O$ (60 mg) using CH_3CN (6 mL) and DMF (3 mL) as the solvent was applied as the top layer for the synthesis and was slowly delivered to the glass tube. The glass tube was then sealed with a cap to prevent evaporation of solvents. The *in-situ* growth of MOF-74(Cu) NS was preceded at room temperature for 12 h in static conditions. After centrifugation, the resulting precipitates were collected and then were washed with DMF and ethanol. The obtained nanomaterials were dried at 353 K under vacuum condition for overnight. The army-green powders were obtained.

2. Fabrication of MOF-74(Cu) NS-GCE the working electrode

A glassy carbon electrode (GCE) with the area electrode of 7.07×10^{-2} cm^2 was polished using 0.3 μm and 0.05 μm alumina slurry on a polishing cloth to create a mirror finish. After that, the electrode was sonicated with absolute ethanol and double-distilled water for about 2 min, respectively. And then it was rinsed thoroughly with double-distilled water and dried under ambient temperature. 1 mg of the as-prepared samples was dispersed into 1 mL solution (Water:ethanol:nafion=12:12:1) to give homogeneous suspension with 10 min bath sonication. Then 10 μL of the suspension of MOF-74(Cu) NS was dip-coated onto GCE surface and dried under an infrared lamp to form MOF-74(Cu) NS-GCE.

3. Characterization of MOF-74(Cu) NS and MOF-74(Cu) NS-CC

SEM images were obtained with a TESCAN MAIA 3 LMH for MOF-74(Cu) NS and VAGA3 (TESCAN, USA) for MOF-74(Cu) NS-CC. The dispersion solutions of MOF-74(Cu) NS samples for TEM measurement were deposited on a carbon film supported by copper grids and TEM images were obtained by a HITACHI HT7700 transmission electron microscope. A tapping mode AFM image was acquired on Bruker NanoScope 3D by directly casting sample dispersion onto mica sheet. XPS data were collected by a Thermo Scientific ESCALAB 250 with an Al Kα source (1486.6 eV). XRD patterns were characterized by a Bruker D8 advance diffractometer with Cu Ka1 radiation (λ=1.5406 Å). FTIR spectra were recorded on a Nicolet 6700 FTIR spectrometer in a KBr pellet, scanning from 4000 to 400 cm^{-1} at room temperature. BET was performed to calculate the surface areas using adsorption data at p/p0 of 0.05-0.3. The total pore volume (Vt) was estimated from the adsorbed amount at p/p0 of 0.995.

4 The assays to detect glucose by MOF-74(Cu) NS-CC

The details for glucose determination were described as fellow:

1 The MOF-74(Cu) NS-CC was cut into 1.0*0.5 cm and fixed on stainless steel electrode holder as working electrode, Ag/AgCl as reference electrode and Pt wire as counter electrode. NaOH (10 mL 0.1 M) was chosen as electrolyte;

2 Cyclic voltammetry (CV) applied to investigate the oxidation and reduction potential of proposed sensor with fellow condition: Scan potential from 0-1.0 V, scan rate 100mV S-1;

3 MOF-74(Cu) NS-CC immersed into NaOH and scan the CV without glucose to get the blank signal;

4 Different concentrations glucose (10 μL) was added into NaOH with magnetic stirring at 150 rpm for 2 min and scan the CV to get the CV curve with target;

5 Chronoamperometry methods were chosen to get the *i-t* curve in glucose concentration determination. The parameters were set as follows: Applied potential: 0.55 V, 0.1 s for per point, 3600 s for duration time. Run the program until the curve reaches a plateau then the glucose (10 μL) was added into NaOH solution from lowest concentration to highest concentration. For each time the glucose added, need to pause the program and stirring for 1 min to disperse the glucose in NaOH then run the program. The time interval between glucose determinations were 30 s.

Fig. S1 Picture showing the spatial arrangement of different liquid layers during the synthesis of MOF-74(Cu) NS-CC.

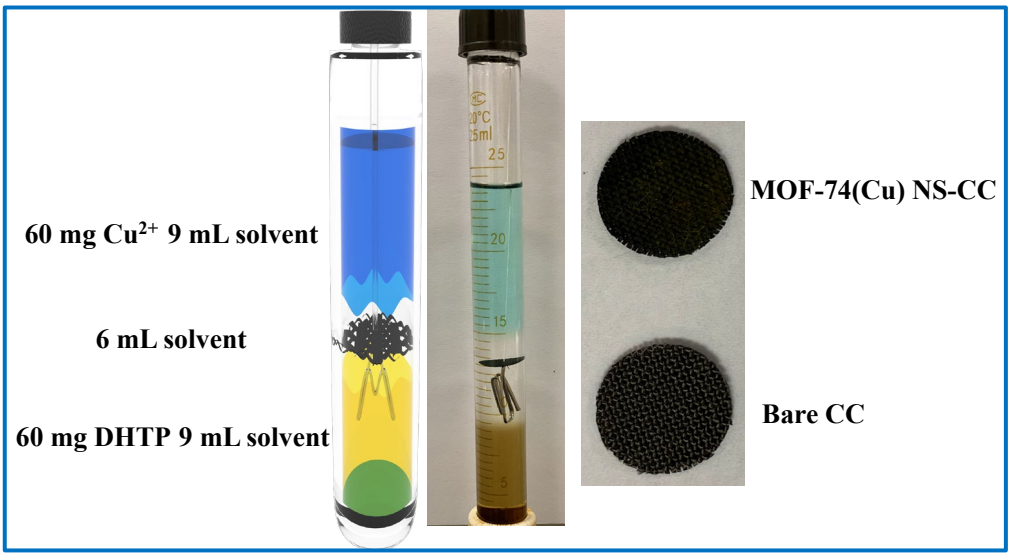

Fig. S2 AFM image of MOF-74(Cu) NS.

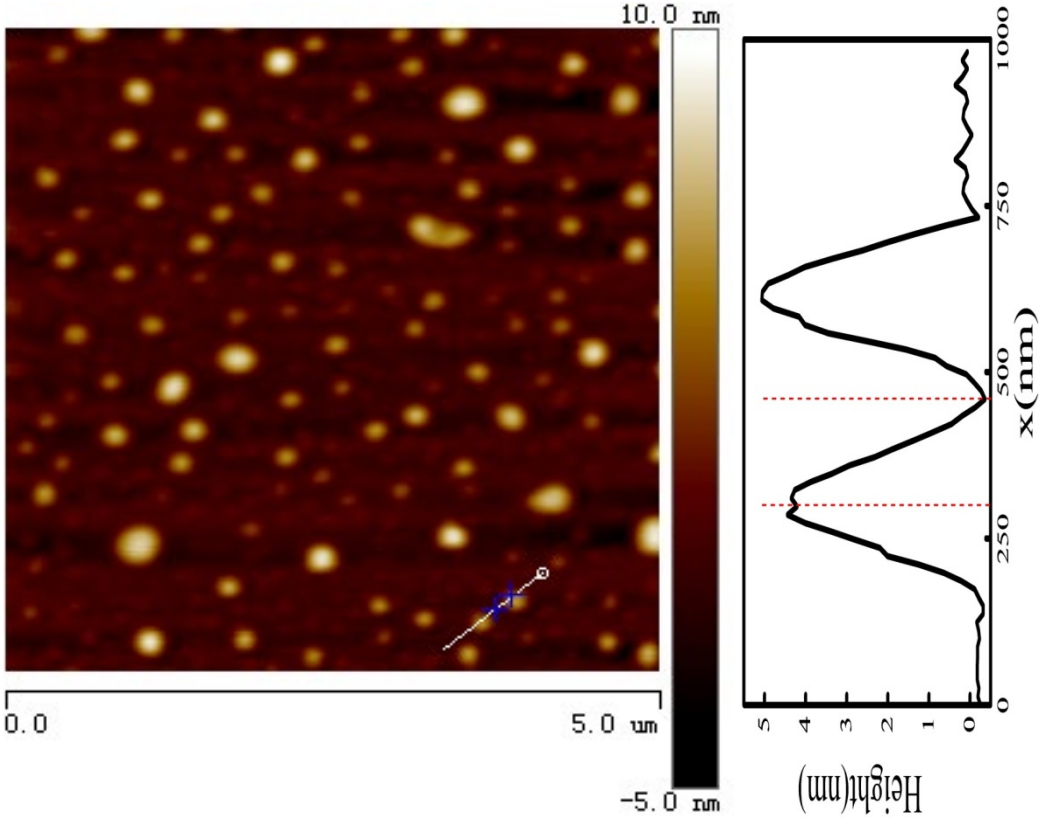

Fig. S3 XRD patterns, FTIR spectra and N_2 adsorption–desorption isotherms of MOF-74(Cu) NS; (A) XRD patterns for MOF-74(Cu) NS; (B) FTIR spectra for MOF-74(Cu) NS; (C) N_2 adsorption-desorption isotherms for MOF-74(Cu) NS.

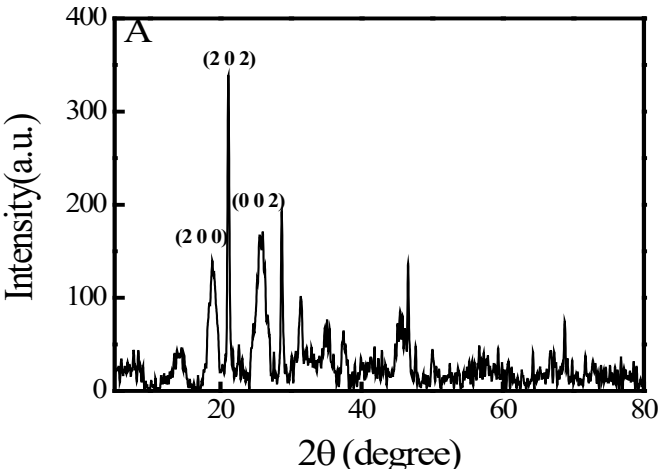

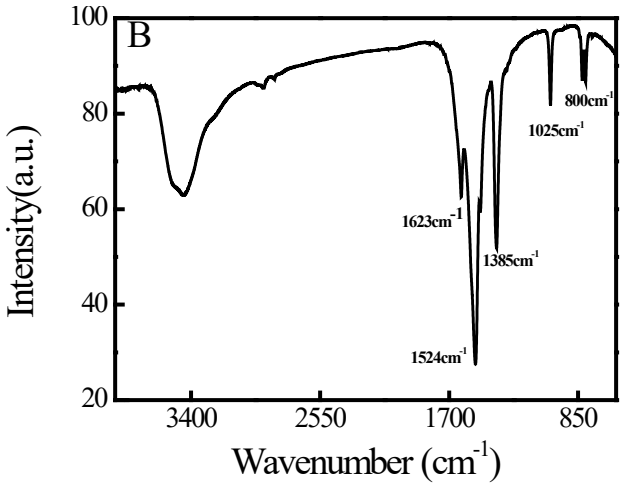

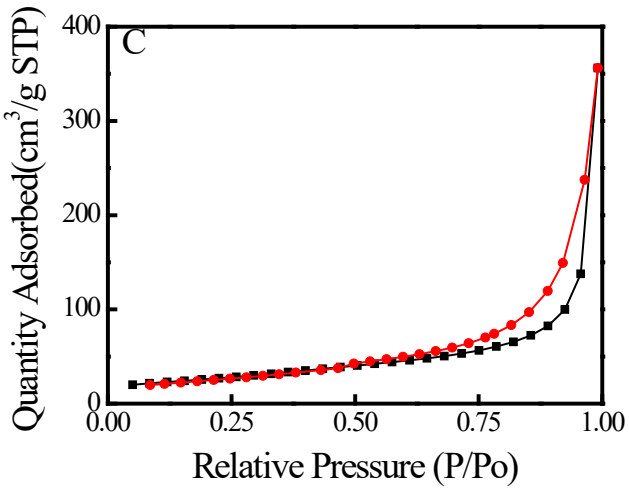

Fig. S4 Stability of the MOF-74(Cu) NS-CC based electrocatalytic sensor. MOF-74(Cu) NS-CC was stored at ambient conditions over 30 days. Data recorded at 0.1 M NaOH with addition of 50 μM glucose at 0.55 V.

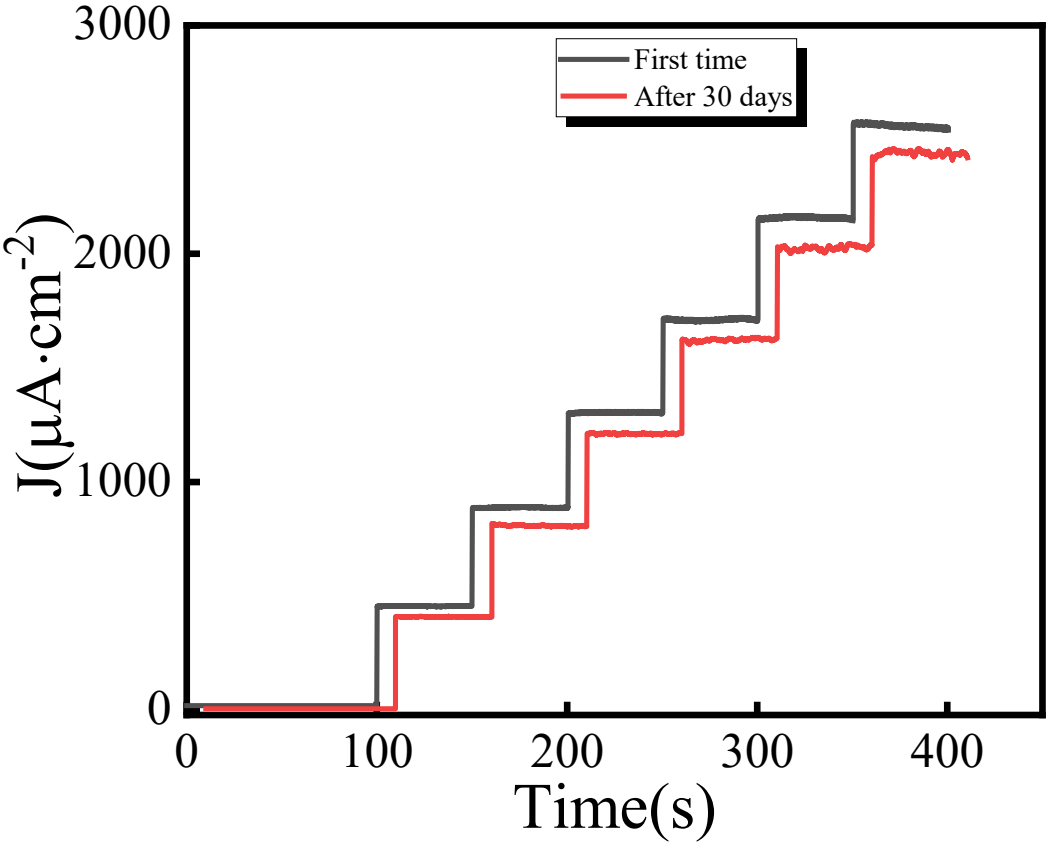

Reference

1 Rodenas T, Luz I, Prieto G, Seoane B, Miro H, Corma A, Kapteijn F, i Xamena FXL, Gascon J (2015) Metal–organic framework nanosheets in polymer composite materials for gas separation. Nat mater 14:48-55